NANO LETTERS
Letter
Cite This: Nano Lett. XXXX, XXX, XXX−XXX
pubs.acs.org/NanoLett

Acid-Assisted Ligand Exchange Enhances Coupling in Colloidal Quantum Dot Solids

Jea Woong Jo,[†,▽,⊥] Jongmin Choi,[†,▽] F. Pelayo García de Arquer,[†,▽] Ali Seifitokaldani,[†] Bin Sun,[†] Younghoon Kim,[†,#] Hyungju Ahn,[‡] James Fan,[†] Rafael Quintero-Bermudez,[†] Junghwan Kim,[†] Min-Jae Choi,[†] Se-Woong Baek,[†] Andrew H. Proppe,[†,§] Grant Walters,[†] Dae-Hyun Nam,[†] Shana Kelley,[§,∥] Sjoerd Hoogland,[†] Oleksandr Voznyy,[†] and Edward H. Sargent*[,†]

[†]Department of Electrical and Computer Engineering, University of Toronto, 10 King's College Road, Toronto, Ontario M5S 3G4, Canada

[‡]Pohang Accelerator Laboratory, Kyungbuk, Pohang 37673, Republic of Korea

[§]Department of Chemistry, University of Toronto, 80 St. George Street, Toronto, Ontario M5S 3G4, Canada

[∥]Department of Pharmaceutical Sciences, Leslie Dan Faculty of Pharmacy, University of Toronto, Toronto, Ontario M5S 3M2, Canada

Supporting Information

ABSTRACT: Colloidal quantum dots (CQDs) are promising solution-processed infrared-absorbing materials for optoelectronics. In these applications, it is crucial to replace the electrically insulating ligands used in synthesis to form strongly coupled quantum dot solids. Recently, solution-phase ligand-exchange strategies have been reported that minimize the density of defects and the polydispersity of CQDs; however, we find herein that the new ligands exhibit insufficient chemical reactivity to remove original oleic acid ligands completely. This leads to low CQD packing and correspondingly low electronic performance. Here we report an acid-assisted solution-phase ligand-exchange strategy that, by enabling efficient removal of the original ligands, enables the synthesis of densified CQD arrays. Our use of hydroiodic acid simultaneously facilitates high CQD packing via proton donation and CQD passivation through iodine. We demonstrate highly packed CQD films with a 2.5 times increased carrier mobility compared with prior exchanges. The resulting devices achieve the highest infrared photon-to-electron conversion efficiencies (>50%) reported in the spectral range of 0.8 to 1.1 eV.

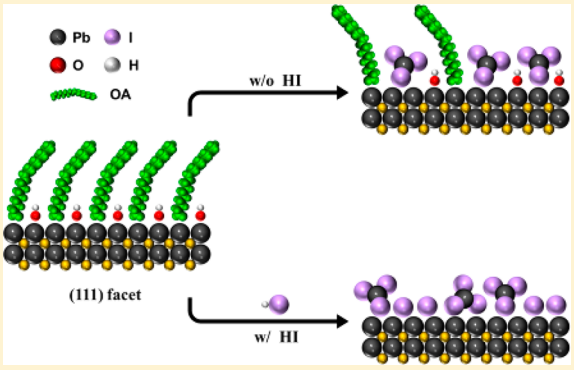

KEYWORDS: *Colloidal quantum dots, photovoltaics, solution-phase ligand exchange, narrow bandgap, infrared, surface passivation*

Colloidal quantum dots (CQDs) are of interest for optoelectronic applications by virtue of their bandgap (E_g) tunable through the quantum size effect as well as for their solution-processing, ambient stability, and uniform film formation without lattice-matching requirements.[1−5] Of chief importance is their ability to harvest energy in the infrared (IR) region of the solar spectrum beyond that absorbed by crystalline silicon (Si) (E_g = 1.1 eV), representing a promising platform to complement Si photovoltaics by providing up to six absolute additional power conversion efficiency (PCE) points on top of those of Si.[6]

Significant improvements in CQD optoelectronic devices have arisen from improved synthesis, surface passivation via ligand exchange, and advanced device strategies.[6−12] Of chief interest for IR applications such as solar energy harvesting, which require large diameter CQDs, is to maximize CQD coupling and overcome the degradation in charge transport that arises when CQD size is increased.[13−16]

Compared with wider-bandgap CQDs used for single-junction solar cells (with E_g = 1.2 to 1.5 eV and particle sizes d = 2.5 to 3.5 nm), CQDs absorbing in the IR range beyond 1.1 eV require diameters d = 4−6 nm.[17,18] The reduced packing density and weak electronic-coupling among dots lead to slower charge transport. Recent studies have shown that the carrier mobilities of CQD solids decrease rapidly to the 4.5 power with CQD radius.[13] IR-CQD solids are projected to possess at least three times lower mobilities than solids based on wider-E_g, smaller-diameter CQDs.

Recently reported solution-phase ligand-exchange strategies—which unlike prior solid-state layer-by-layer approaches replace quantum dot ligands while still dispersed as colloids—

Received: April 12, 2018
Revised: May 25, 2018
Published: June 18, 2018

DOI: 10.1021/acs.nanolett.8b01470
Nano Lett. XXXX, XXX, XXX−XXX

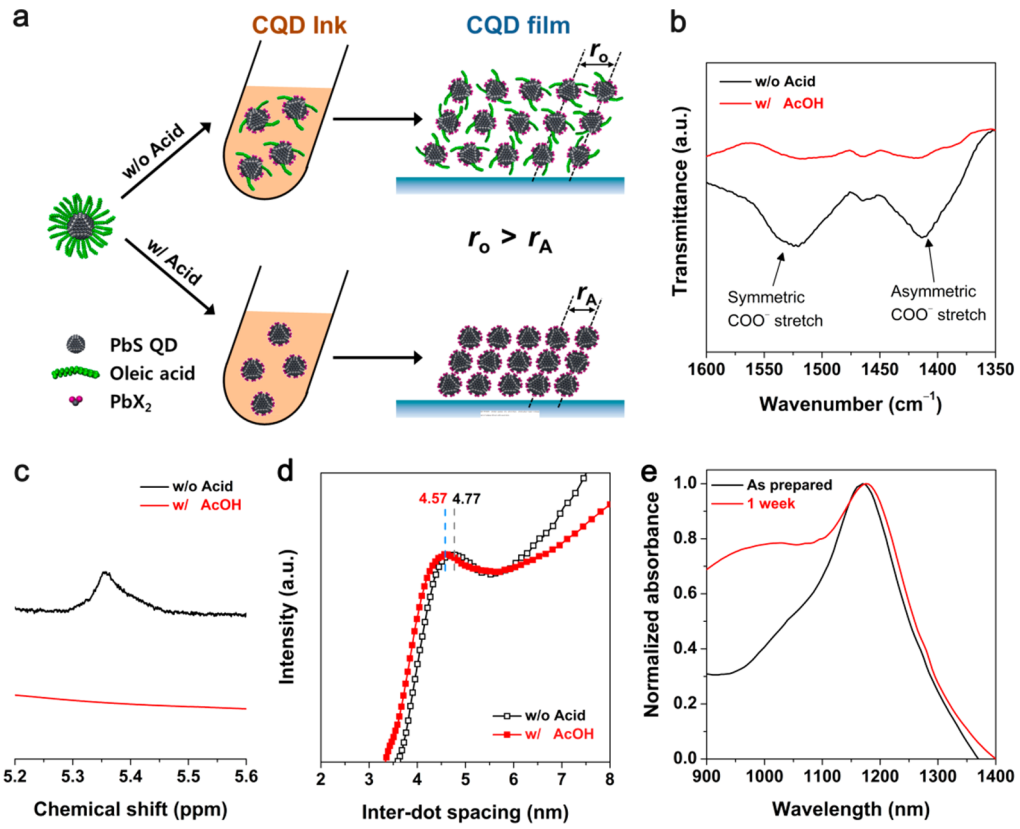

Figure 1. Acid-assisted solution-phase ligand exchange for the densification of IR-CQD films. (a) Schematic illustration of conventional and acid-assisted solution-phase ligand exchange methods for IR-CQDs. (b) FT-IR spectra (wavenumber range = 1600−1350 cm^{-1}), (c) ^1H NMR spectra, and (d) distribution of interdot spacing between dots of IR-CQD films (E_g = 1.08 eV) prepared without and with AcOH. (e) Absorption spectra of IR-CQD films prepared with AcOH before and after storage in air for 1 week.

offer practical advantages in optoelectronic applications because they minimize density of defects and preserve the size distribution of the CQD population.[9,10] However, present-day solution-phase ligand exchanges exhibit insufficient chemical reactivity, especially for large-diameter infrared CQDs.[7,8,12] An appreciable fraction of the original ligands remain at the CQD surface, and the increased steric hindrance ultimately leads to suboptimally packed QD films with poor electronic coupling. To date, the demonstration of a solution-exchange strategy that maximizes CQD coupling without sacrificing passivation has remained elusive.

Here we report a solution-phase ligand-exchange method that, by including hydrohalic acid additives, simultaneously achieves a more complete surface exchange, which we show leads to a greater packing density and a higher mobility, and superior passivation. We found that introducing acids during ligand exchange promotes the release of the original oleic acid insulating ligands, enabling compact IR-CQD solids with improved mobility; however, this early exchange also sacrificed surface passivation. Guided by computational simulations, we then designed a strategy that, by employing hydroiodic acid, provides dense and well-passivated IR-CQDs solids. We achieve infrared solar cells with a record PCE after a simulated Si solar cell filter (Si-filtered PCE) of 0.9% for CQD bandgaps in the range of 0.8 to 1.1 eV.

In recently developed solution-phase ligand exchanges for CQD inks, reagents such as CH_3NH_3I and PbI_2 have been used to remove oleic acid (OA) and to provide passivation of the CQD surface (Figure 1a).[9−12] However, because of the moderate reactivity of these chemicals, the bulky OA ligands are not fully removed, and a partial layer of OA remains on the surface of CQDs following ligand exchange.[12] As a result, the final CQD films exhibit increased interdot spacings, weakened electronic coupling, and reduced mobilities. This effect is particularly acute in large-diameter CQDs, where the diminished spillover of electron/hole wave functions corresponds to weakened interdot coupling.[13]

The excess residual OA ligands required removal to increase the mobility of CQD films. We hypothesized that the addition of acidic species that could provide additional protons during the ligand-exchange reaction would mediate and facilitate the detachment of OA ligands.[19−21] This would enable the assembly of compact CQD films that would not be subject to the steric repulsion of OA ligands.[22−24]

We first explored the introduction of additional acids during solution-phase ligand exchanges. The first candidate was acetic acid (AcOH), which has the same functional group as OA (i.e., carboxylic acid group) but exhibits a higher electronegativity and hence a higher acidity. The solution-phase ligand exchange was carried out following a previously reported method for lead halide (PbX_2)-passivated IR-CQD inks (see the Experimental Section in the Supporting Information).[7,8,25] The acid additive was injected into the solution before vortexing the nonpolar/polar biphasic mixture for the transfer of the CQDs from octane to *N*,*N*-dimethylmethanamide (DMF) solvents. During ligand exchange, we found that acetic acid greatly accelerates the phase transfer of IR-CQDs into DMF. We attributed this to the enhanced release of OA

DOI: 10.1021/acs.nanolett.8b01470
Nano Lett. XXXX, XXX, XXX−XXX

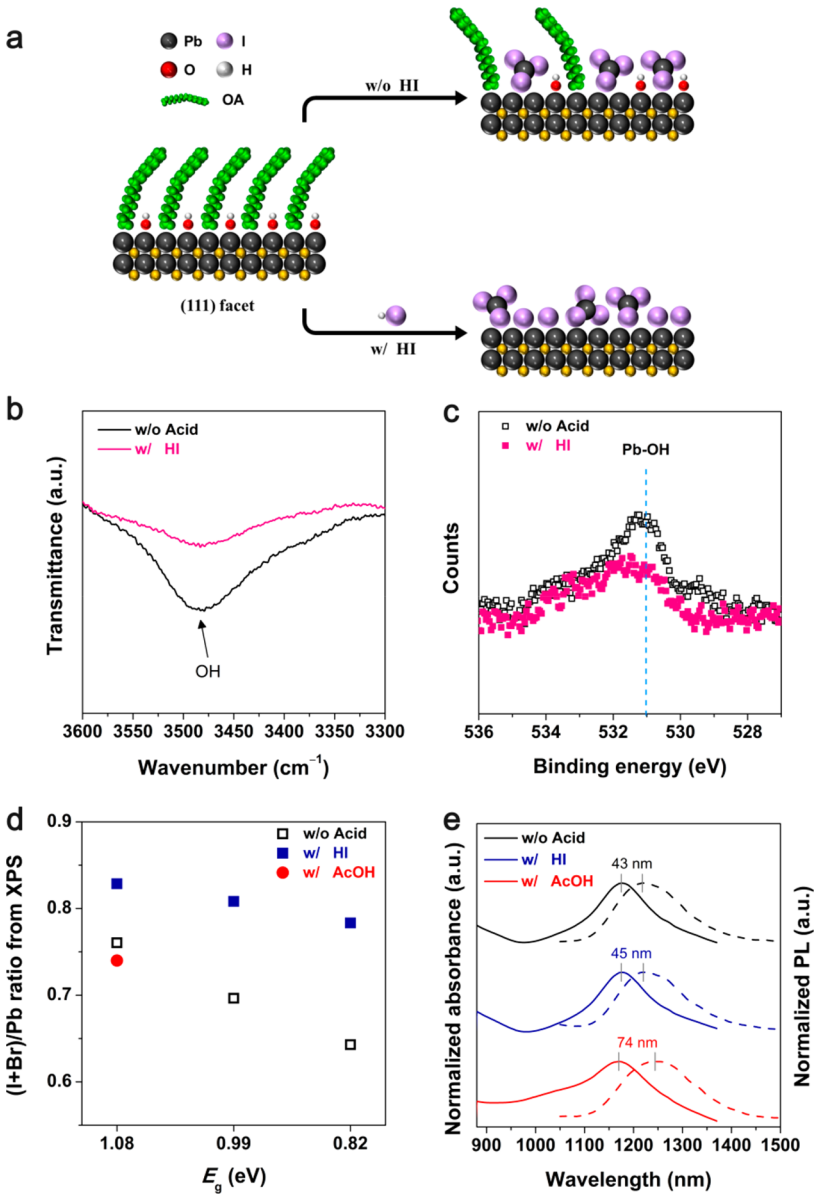

Figure 2. Surface passivation of IR-CQDs as a function of acid additive used in solution-phase ligand exchange. (a) Schematic illustration of HI-assisted solution-phase ligand exchange on the (111) facets of PbS CQDs. (b) FT-IR spectra (wavenumber range = 3600−3300 cm^{-1}) and (c) O 1s XPS spectra of IR-CQD films (E_g = 1.08 eV) prepared without and with HI additive. (d) (I+Br)/Pb atomic ratio measured from XPS of IR-CQD films prepared without and with HI additive. (e) Absorption and PL spectra of IR-CQD films prepared using different acid additives.

ligands from the surface of CQDs enabled by the additional proton sources (Figure S1).

The chemical structure of CQDs before and after AcOH acid addition was investigated using Fourier-transform infrared spectroscopy (FT-IR) (Figure 1b and FigureS2). CQD films prepared without acid additives showed strong peaks for the range of asymmetric −COO− and symmetric −COO− stretch vibrations, revealing the existence of residual OA ligands following ligand exchange. In contrast, the signals associated with OA ligands were not detected in CQD films prepared with acid additives, indicating that the OA ligands on the surface of CQDs are substantially completely removed in the presence of acids during solution-phase ligand exchange. Additional ^{1}H NMR spectroscopy confirmed this picture (Figure 1c). Compared with control samples without acid additives, IR-CQDs prepared with AcOH showed the reduced intensity at 5.5 to 5.6 ppm associated with the proton on the C═C bond of OA.

The packing density of IR-CQD films was evaluated by performing grazing incidence X-ray diffraction (GIXRD) measurements (Figure 1d). Films assembled from acid-exchanged CQDs showed a reduction in the interdot spacing (the center-to-center distance among CQDs) of up to 0.2 nm compared with those made using the standard exchange. This result demonstrates the improved densification of CQD films induced by the controlled presence of acids during ligand exchange.

To evaluate the stability of IR-CQD films based on solution exchange with AcOH additives, we monitored the width and position of the exciton absorption by UV−vis spectroscopy (Figure 1e). After films were exposed to air for 1 week, the exciton peak broadened, pointing to the degradation of AcOH-

DOI: 10.1021/acs.nanolett.8b01470
Nano Lett. XXXX, XXX, XXX−XXX

treated IR-CQDs through accelerated etching and fusion mechanisms.

To investigate further the ligand-exchange mechanism and gain further insight into the CQD surfaces in the presence of AcOH additives, we turned to density functional theory (DFT) calculations.[26−30] We considered a CQD (111) facet composed of Pb atoms (Figure 2a) capped by OA and OH groups, a picture that agrees with previous works.[31,32] Whereas AcOH was found experimentally to remove the majority of OA, calculations predict that it can also remove existing OH groups on the CQD surfaces (Table 1). Because AcOH does not offer additional halide passivation (Figure 2d), we propose that this removal of the OH group by the addition of AcOH may increase the exposure of facets, favoring CQD aggregation.

Table 1. Reaction Energy Differences with Acid Additives on the (111) Facet of PbS IR-CQDs Calculated from DFT Simulation[a]

reaction[b]	ΔE_{DFT}^{rxn} (eV)	ΔG^{rxn} (eV)
*OH + HI → *I + H_2O	−1.082	−1.056
*AcO + HI → *I + AcOH	−0.736	−0.526
*OH + AcOH → *AcO + H_2O	−0.375	−0.559

[a]For simplifying the calculation, long OA ligands were replaced with short acetate molecules (CH_3COO^-). [b]All adsorbents including *OH, *AcO, and *I were considered on the Pb (111) facet on the QD (*).

We reasoned that an efficient acid-aided exchange would require the acid additive to replace simultaneously the OA and OH groups and provide surface passivation. Given the known affinity of halide groups for CQD surfaces,[33−36] we turned our attention to hydrohalic acids. Hydroiodic acid (HI) was chosen as an alternative to AcOH in view of the strong binding energy of iodide to the surface of PbS CQDs.[33] DFT calculations for HI confirmed this scenario, showing a favored energy landscape for both CH_3COO^- (with ΔG^{rxn} = −0.526 eV) and OH (with ΔG^{rxn} = −1.056 eV) replacement and for rendering a stable halide-rich Pb-passivated surface (Table 1). This was verified experimentally using FT-IR and XPS measurements, which showed a diminished presence of OH groups (Figure 2b,c).

The superior passivation facilitated by the HI exchange was further confirmed through XPS, which revealed an increased proportion of halide species (ratioed to Pb) for a range of CQD sizes (Figure 2d). CQDs prepared with HI showed an increased halide presence compared with CQDs without acid and with AcOH. This indicates that HI-assisted CQD exchange can also provide iodide passivation, preventing CQD aggregation, fusion, and exposure to oxidizing agents.

The improved passivation using HI additives was further verified by smaller Stokes shifts calculated from absorption and photoluminescence spectra (Figure 2e). HI-treated CQDs provided similar Stokes shifts, of ∼45 nm, compared with OA-rich control samples (Stokes shift = 43 nm). AcOH-treated CQDs, on the contrary, showed significantly increased Stokes shifts of 74 nm. This suggests that the adverse energy broadening that arises from CQD fusing and etching during ligand exchange in a proton-rich environment is suppressed via the use of HI.[37] Compared with CQD films prepared with and without HI additive, AcOH-treated CQD films showed lower photoluminescence, suggesting an increased trap density in these materials (Figure S4f).

We then sought to evaluate the packing of CQD films of different sizes exchanged with HI additives. Both FT-IR and GIXRD reveal that HI is also able to induce denser packing of CQD films (Figures S2 and S3). This trend is observed for various CQD sizes, with bandgaps in the range of 0.82 to 1.08 eV (Figure 3a), showcasing the benefit of this method as the size of the CQDs increases.

To characterize the mobility of IR-CQD films, we carried out field-effect transistor (FET) measurements. FET devices were fabricated using a bottom-gate, top-contact configuration, where Ti and ZrO_2 were deposited as gate and dielectric layers, respectively (see the Experimental Section in the Supporting Information).[38] The transfer characteristics of CQD FETs (E_g = 1.08 eV) show a 2.5 times increase in the electron mobility (0.028 $cm^2\ V^{-1}\ s^{-1}$) for acid-exchanged dots compared with control films (0.011 $cm^2\ V^{-1}\ s^{-1}$) (Figure 3b).

We then built solar cells employing the HI-treated CQDs (Figure 4a and Figure S6). The device architecture consisted of indium tin oxide (ITO)/zinc oxide (ZnO)/CQD/1,2-ethanedithiol-treated CQD/Au.[39] The $J-V$ characteristics under Si-filtered AM 1.5G solar illumination of control and HI-treated solar cells showcase the benefits of the latter (Figure S5).[6−8] Adding HI contributed to the enhancement of J_{SC}, which is due to the densification of the CQD layer: The highest J_{SC} values of CQD devices for E_g of 1.08, 0.99, and 0.82 eV were increased from 3.07, 2.83, and 3.10 mA cm^{-2} to 3.19, 3.39, and 4.48 mA cm^{-2} after introducing the HI additive. The

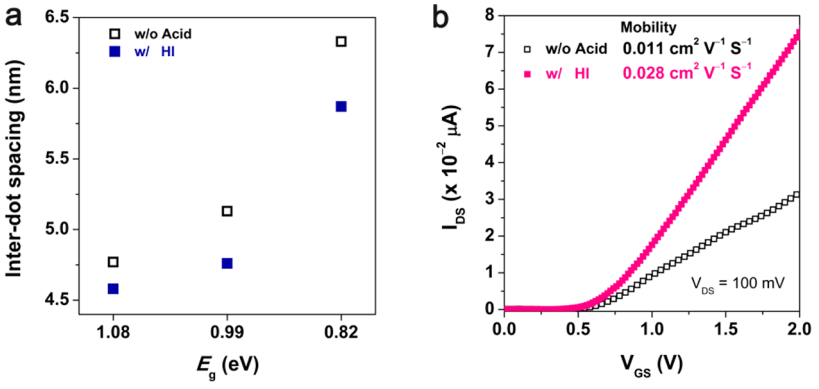

Figure 3. Mobility of IR-CQD films prepared with HI additive during solution-phase ligand exchange compared with controls. (a) Distribution of interdot spacing between dots of IR-CQD films without and with HI additive. (b) Transfer characteristics of FETs fabricated using IR-CQDs (E_g = 1.08 eV) without and with HI additive.

DOI: 10.1021/acs.nanolett.8b01470
Nano Lett. XXXX, XXX, XXX−XXX

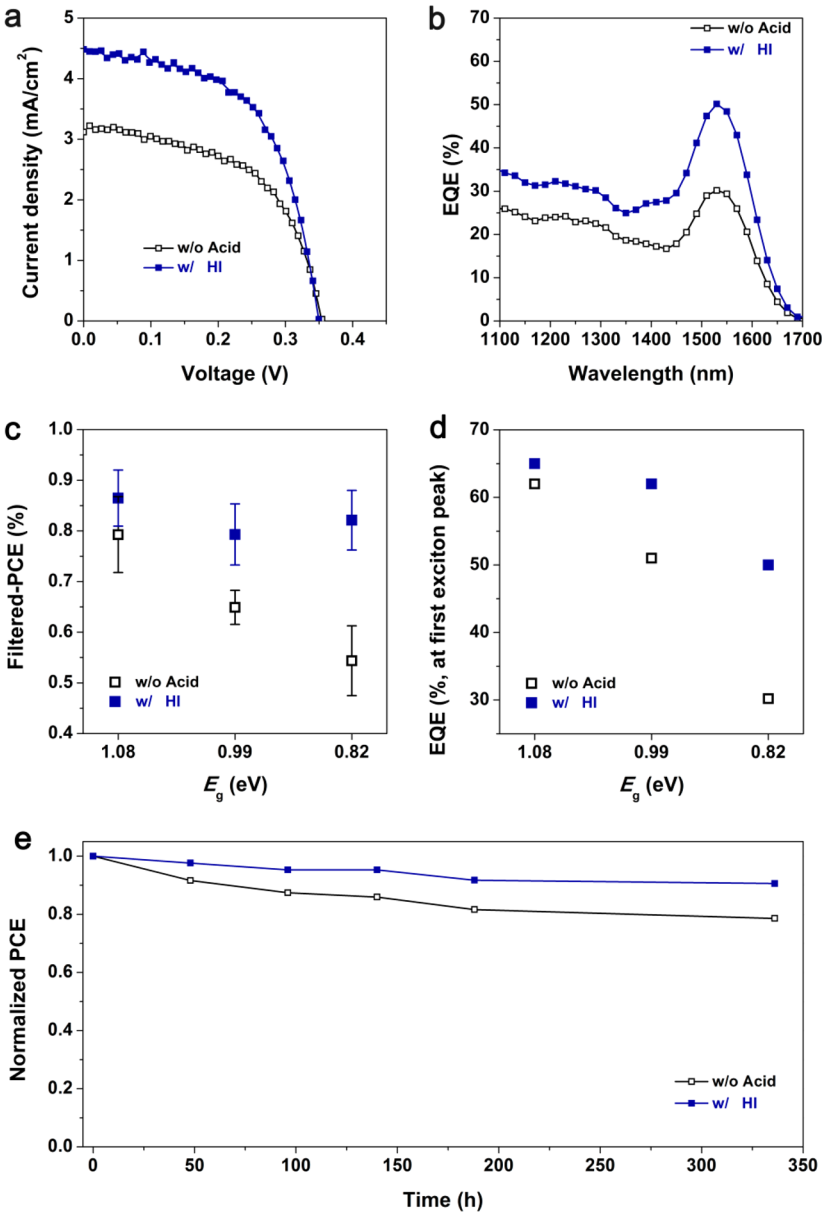

Figure 4. Performance of IR-CQD solar cells prepared using HI additive compared with controls. (a) Si-filtered $J-V$ curves and (b) EQE spectra of IR-CQD solar cells (E_g = 0.82 eV) prepared without and with HI additive. (c) Filtered-PCE values and (d) EQE values at first exciton peaks of IR-CQD solar cells prepared without and with HI additive for E_g of (a) 1.08, (b) 0.99, and (c) 0.82 eV. (e) Filtered-PCE changes of the IR-CQD solar cells as a function of exposure time to air at room temperature.

denser packing and improved transport enabled by the HI additive also led to an increase in fill factor (FF). Because the V_{OC} of CQD solar cells was preserved under the HI treatment, Si-filtered PCEs over 0.85% for CQDs with excitons in the range of 0.82 to 1.08 eV, previously unattained with legacy CQD inks, have been demonstrated (Figure 4c). These represent the highest PCE values among solution-processed IR solar cells reported to date.[6−8,40] When the devices were measured under full AM1.5G spectrum, HI-treated solar cells also showed improved performance compared with control devices (Table S1).

Notably, the devices exhibit remarkably high external quantum efficiencies (EQEs) (Figure 4b). For CQDs with a 1550 nm exciton peak, a 50% EQE is obtained, in contrast with <30% for control samples. This trend holds for other CQD bandgaps (Figure 4d and Figure S8), showcasing the beneficial impact of HI-promoted exchange for infrared optoelectronic sensing applications beyond photovoltaics.

We then tested the air stability of unencapsulated CQD solar cells. We found that devices using HI retain ∼90% of their initial PCE after an initial study of 300 h under air storage without encapsulation, indicating promising environmental stability in the CQD solar cells prepared using the hydrohalic method (Figure 4e).

In summary, the present work demonstrates the benefits of acid-promoted ligand exchange for CQDs in the solution phase. We observed that acid additives help to remove residual OA ligands on the surfaces of CQDs, ligands not fully detached using previously reported ligand-exchange methods. This enables the realization of densely packed CQD films due to the absence of steric repulsions associated with bulky OA ligands. In particular, we found that hydrohalic acids such as

DOI: 10.1021/acs.nanolett.8b01470
Nano Lett. XXXX, XXX, XXX−XXX

HI can simultaneously provide dense packing and efficient CQD passivation as abundant OH groups at the CQD surface are replaced by I passivants. This works against CQD fusion during ligand exchange. Only by using this method were we able to achieve high Si-filtered PCEs of ∼0.9% and high EQEs of 50% at 1550 nm. Our study demonstrates a new route to achieve highly compact, well-passivated CQD films that, with improved charge-transport properties, enable the realization of efficient infrared optoelectronic devices.

■ ASSOCIATED CONTENT

Supporting Information

The Supporting Information is available free of charge on the ACS Publications website at DOI: 10.1021/acs.nanolett.8b01470.

Experimental section, FT-IR, XPS, distribution of interdot spacing, solar cell parameters of IR-CQD solar cells depending on additives during solution-phase ligand exchange, and EQE data (PDF)

■ AUTHOR INFORMATION

Corresponding Author

*E-mail: ted.sargent@utoronto.ca.

ORCID

Jea Woong Jo: 0000-0001-8086-2644
Ali Seifitokaldani: 0000-0002-7169-1537
Younghoon Kim: 0000-0003-0860-2156
James Fan: 0000-0002-1594-865X
Rafael Quintero-Bermudez: 0000-0002-4233-395X
Grant Walters: 0000-0002-9005-2335
Shana Kelley: 0000-0003-3360-5359
Oleksandr Voznyy: 0000-0002-8656-5074
Edward H. Sargent: 0000-0003-0396-6495

Present Addresses

⊥J.W.J.: Department of Energy and Materials Engineering, Dongguk University-Seoul, 04620 Seoul, Republic of Korea.
#Y.K.: Convergence Research Center for Solar Energy, Daegu Gyeongbuk Institute of Science and Technology, Daegu 42988, Republic of Korea.

Author Contributions

▽J.W.J., J.C., and F.P.G.d.A contributed equally to this work.

Notes

The authors declare no competing financial interest.

■ ACKNOWLEDGMENTS

This work was supported by the Ontario Research Fund-Research Excellence program (ORF-RE7 ministry of Research and Innovation, Ontario Research Fund-Research Excellence Round 7) and by the Natural Sciences and Engineering Research Council (NSERC) of Canada. All DFT computations were performed on the IBM BlueGene/Q supercomputer with support from the Southern Ontario Smart Computing Innovation Platform (SOSCIP, SOSCIP is funded by the Federal Economic Development Agency of Southern Ontario, the Province of Ontario, IBM Canada Ltd., Ontario Centres of Excellence, Mitacs and 15 Ontario academic member institutions). A.S. thanks Fonds de Recherche du Quebec - Nature et Technologies (FRQNT) for support in the form of a postdoctoral fellowship award. We thank L. Levina, R. Wolowiec, D. Kopilovic, and E. Palmiano for their help over the course of this research.

■ REFERENCES

(1) Colvin, V. L.; Schlamp, M. C.; Alivisatos, A. P. *Nature* **1994**, *370*, 354−357.
(2) Sargent, E. H. *Nat. Photonics* **2009**, *3*, 325−331.
(3) Kovalenko, M. V.; Scheele, M.; Talapin, D. V. *Science* **2009**, *324*, 1417−1420.
(4) Konstantatos, G.; Howard, I.; Fischer, A.; Hoogland, S.; Clifford, J.; Klem, E.; Levina, L.; Sargent, E. H. *Nature* **2006**, *442*, 180−183.
(5) Kramer, I. J.; Sargent, E. H. *Chem. Rev.* **2014**, *114*, 863−882.
(6) Ip, A. H.; Kiani, A.; Kramer, I. J.; Voznyy, O.; Movahed, H. F.; Levina, L.; Adachi, M. M.; Hoogland, S.; Sargent, E. H. *ACS Nano* **2015**, *9*, 8833−8842.
(7) Kiani, A.; Sutherland, B. R.; Kim, Y.; Ouellette, O.; Levina, L.; Walters, G.; Dinh, C. T.; Liu, M.; Voznyy, O.; Lan, X.; Labelle, A. J.; Ip, A. H.; Proppe, A.; Ahmed, G. H.; Mohammed, O. F.; Hoogland, S.; Sargent, E. H. *Appl. Phys. Lett.* **2016**, *109*, 183105.
(8) Fan, J. Z.; Liu, M.; Voznyy, O.; Sun, B.; Levina, L.; Quintero-Bermudez, R.; Liu, M.; Ouellette, O.; García de Arquer, F. P. G.; Hoogland, S.; Sargent, E. H. *ACS Appl. Mater. Interfaces* **2017**, *9*, 37536−37541.
(9) Liu, M.; Voznyy, O.; Sabatini, R.; García de Arquer, F. P.; Munir, R.; Balawi, A. H.; Lan, X.; Fan, F.; Walters, G.; Kirmani, A. R.; Hoogland, S.; Laquai, F.; Amassian, A.; Sargent, E. H. *Nat. Mater.* **2017**, *16*, 258−263.
(10) Ning, Z.; Dong, H.; Zhang, Q.; Voznyy, O.; Sargent, E. H. *ACS Nano* **2014**, *8*, 10321−10327.
(11) Yang, Z.; Janmohamed, A.; Lan, X.; García de Arquer, F. P.; Voznyy, O.; Yassitepe, E.; Kim, G.-H.; Ning, Z.; Gong, X.; Comin, R.; Sargent, E. H. *Nano Lett.* **2015**, *15*, 7539−7543.
(12) Jo, J. W.; Kim, Y.; Choi, J.; De Arquer, F. P. G.; Walters, G.; Sun, B.; Ouellette, O.; Kim, J.; Proppe, A. H.; Quintero-Bermudez, R.; Fan, J.; Xu, J.; Tan, C. S.; Voznyy, O.; Sargent, E. H. *Adv. Mater.* **2017**, *29*, 1703627.
(13) Yazdani, N.; Bozyigit, D.; Yarema, O.; Yarema, M.; Wood, V. *J. Phys. Chem. Lett.* **2014**, *5*, 3522−3527.
(14) Shabaev, A.; Efros, A. L.; Efros, A. L. *Nano Lett.* **2013**, *13*, 5454−5461.
(15) Bozyigit, D.; Lin, W. M. M.; Yazdani, N.; Yarema, O.; Wood, V. *Nat. Commun.* **2015**, *6*, 6180.
(16) Gilmore, R. H.; Lee, E. M. Y.; Weidman, M. C.; Willard, A. P.; Tisdale, W. A. *Nano Lett.* **2017**, *17*, 893−901.
(17) Moreels, I.; Lambert, K.; Smeets, D.; De Muynck, D.; Nollet, T.; Martins, J. C.; Vanhaecke, F.; Vantomme, A.; Delerue, C.; Allan, G.; Hens, Z. *ACS Nano* **2009**, *3*, 3023−3030.
(18) Weidman, M. C.; Beck, M. E.; Hoffman, R. S.; Prins, F.; Tisdale, W. A. Monodisperse. *ACS Nano* **2014**, *8*, 6363−6371.
(19) Balazs, D. M.; Dirin, D. N.; Fang, H.-H.; Protesescu, L.; ten Brink, G. H.; Kooi, B. J.; Kovalenko, M. V.; Loi, M. A. *ACS Nano* **2015**, *9*, 11951−11959.
(20) Zarghami, M. H.; Liu, Y.; Gibbs, M.; Gebremichael, E.; Webster, C.; Law, M. *ACS Nano* **2010**, *4*, 2475−2485.
(21) Aldana, J.; Lavelle, N.; Wang, Y.; Peng, X. *J. Am. Chem. Soc.* **2005**, *127*, 2496−2504.
(22) Zarghami, M. H.; Liu, Y.; Gibbs, M.; Gebremichael, E.; Webster, C.; Law, M. *ACS Nano* **2010**, *4*, 2475−2485.
(23) Sun, L.; Choi, J. J.; Stachnik, D.; Bartnik, A. C.; Hyun, B.-R.; Malliaras, G. G.; Hanrath, T.; Wise, F. W. *Nat. Nanotechnol.* **2012**, *7*, 369−373.
(24) Brown, P. R.; Kim, D.; Lunt, R. R.; Zhao, N.; Bawendi, M. G.; Grossman, J. C.; Bulović, V. *ACS Nano* **2014**, *8*, 5863−5872.
(25) Kim, Y.; Che, F.; Jo, J. W.; Choi, J.; Voznyy, O.; De Arquer, F. P. G.; Sun, B.; Kim, J.; Quintero-Bermudez, R.; Fan, F.; Tan, C. S.; Bladt, E.; Walters, G.; Proppe, A.; Zou, C.; Yuan, H.; Bals, S.; Hofkens, J.; Roeffaers, M. B. J.; Sargent, E. H. **2018**, submitted *Nat. Commun.*.

DOI: 10.1021/acs.nanolett.8b01470
Nano Lett. XXXX, XXX, XXX−XXX

(26) VandeVondele, J.; Krack, M.; Mohamed, F.; Parrinello, M.; Chassaing, T.; Hutter, J. *Comput. Phys. Commun.* **2005**, *167*, 103−128.
(27) Perdew, J. P.; Burke, K.; Ernzerhof, M. *Phys. Rev. Lett.* **1996**, *77*, 3865−3868.
(28) Lippert, G.; Hutter, J.; Parrinello, M. *Mol. Phys.* **1997**, *92*, 477−488.
(29) Hartwigsen, C.; Goedecker, S.; Hutter, J. *Phys. Rev. B: Condens. Matter Mater. Phys.* **1998**, *58*, 3641−3662.
(30) VandeVondele, J.; Hutter, J. *J. Chem. Phys.* **2007**, *127*, 114105.
(31) Zherebetskyy, D.; Scheele, M.; Zhang, Y.; Bronstein, N.; Thompson, C.; Britt, D.; Salmeron, M.; Alivisatos, P.; Wang, L.-W. *Science* **2014**, *344*, 1380−1384.
(32) Cao, Y.; Stavrinadis, A.; Lasanta, T.; So, D.; Konstantatos, G. *Nature Energy* **2016**, *1*, 16035.
(33) Ning, Z.; Voznyy, O.; Pan, J.; Hoogland, S.; Adinolfi, V.; Xu, J.; Li, M.; Kirmani, A. R.; Sun, J.; Minor, J.; Kemp, K. W.; Dong, H.; Rollny, L.; Labelle, A.; Carey, G.; Sutherland, B. R.; Hill, I.; Amassian, A.; Liu, H.; Tang, J.; Bakr, O. M.; Sargent, E. H. *Nat. Mater.* **2014**, *13*, 822−828.
(34) Ip, A. H.; Thon, S. M.; Hoogland, S.; Voznyy, O.; Zhitomirsky, D.; Debnath, R.; Levina, L.; Rollny, L. R.; Carey, G. H.; Fischer, A.; Kemp, K. W.; Kramer, I. J.; Ning, Z.; Labelle, A. J.; Chou, K. W.; Amassian, A.; Sargent, E. H. *Nat. Nanotechnol.* **2012**, *7*, 577−582.
(35) Lan, X.; Voznyy, O.; Kiani, A.; García de Arquer, F. P.; Abbas, A. S.; Kim, G. H.; Liu, M.; Yang, Z.; Walters, G.; Xu, J.; Yuan, M.; Ning, Z.; Fan, F.; Kanjanaboos, P.; Kramer, I. J.; Zhitomirsky, D.; Lee, P.; Perelgut, A.; Hoogland, S.; Sargent, E. H. *Adv. Mater.* **2016**, *28*, 299−304.
(36) Lan, X.; Voznyy, O.; García de Arquer, F. P.; Liu, M.; Xu, J.; Proppe, A. H.; Walters, G.; Fan, F.; Tan, H.; Liu, M.; Yang, Z.; Hoogland, S.; Sargent, E. H. *Nano Lett.* **2016**, *16*, 4630−4634.
(37) Voznyy, O.; Levina, L.; Fan, F.; Walters, G.; Fan, J. Z.; Kiani, A.; Ip, A. H.; Thon, S. M.; Proppe, A. H.; Liu, M.; Sargent, E. H. *Nano Lett.* **2017**, *17*, 7191−7195.
(38) Sun, B.; Voznyy, O.; Tan, H.; Stadler, P.; Liu, M.; Walters, G.; Proppe, A. H.; Liu, M.; Fan, J.; Zhuang, T.; Li, J.; Wei, M.; Xu, J.; Kim, Y.; Hoogland, S.; Sargent, E. H. *Adv. Mater.* **2017**, *29*, 1700749.
(39) Chuang, C.-H. M.; Brown, P. R.; Bulović, V.; Bawendi, M. G. *Nat. Mater.* **2014**, *13*, 796−801.
(40) Bi, Y.; Pradhan, S.; Gupta, S.; Akgul, M. Z.; Stavrinadis, A.; Konstantatos, G. *Adv. Mater.* **2018**, *30*, 1704928.

DOI: 10.1021/acs.nanolett.8b01470
Nano Lett. XXXX, XXX, XXX−XXX